International Journal of Medical, Medicine and Health Sciences
ISSN: 2517-9969
Vol:11, No:4, 2017

Fall Avoidance Control of Wheeled Inverted Pendulum Type Robotic Wheelchair While Climbing Stairs

Nan Ding, Motoki Shino, Nobuyasu Tomokuni, Genki Murata

***Abstract*—**The wheelchair is the major means of transport for physically disabled people. However, it cannot overcome architectural barriers such as curbs and stairs. In this paper, the authors proposed a method to avoid falling down of a wheeled inverted pendulum type robotic wheelchair for climbing stairs. The problem of this system is that the feedback gain of the wheels cannot be set high due to modeling errors and gear backlash, which results in the movement of wheels. Therefore, the wheels slide down the stairs or collide with the side of the stairs, and finally the wheelchair falls down. To avoid falling down, the authors proposed a slider control strategy based on skyhook model in order to decrease the movement of wheels, and a rotary link control strategy based on the staircase dimensions in order to avoid collision or slide down. The effectiveness of the proposed fall avoidance control strategy was validated by ODE simulations and the prototype wheelchair.

***Keywords*—**EPW, fall avoidance control, skyhook, wheeled inverted pendulum.

I. Introduction

IN Japan and the United States, the number of physically disabled people is predicted to increase every year along with the aging. There were about 3.9 million physically disabled people living at home by 2011 in Japan, whose major means of transport is wheelchair [1]. In the US, the population using wheeled mobility devices were about 3.3 million [2]. Since social activities are effective to improve their quality of life, it is necessary to provide them with mobility devices. Although plenty of researches on electrically-powered wheelchair(EPW) were conducted, there is still a signifcant shortcoming that the indoor EPWs are limited for outdoor use. EPW users may fall over when driving in road conditions such as uneven terrains and steep hills, and they cannot access some areas due to architectural barriers such as curbs and stairs.

In order to enable EPWs to move freely, one of the methods is to create an environment with no architectural barriers by using elevators, slopes, etc. Another way is to develop an EPW option which enables it to climb up and down stairs. In Japan, architectual barriers in communal facilities are banned by the Barrier-free Law. However, the law is not applied to residential facilities. Similarly, there are also some places where the Americans with Disablilies Act Accessibility Guidelines (ADAAG) [3] criteria are not met. Actually, it is impossible to remove all barriers due to the costs and spaces.

In this study, the authors focusd on second way and proposed a mechanism and control method of EPW for stair-climbing.

N. Ding is with the Guraduate School of Frontier Science, The University of Tokyo, Tokyo, Japan. 5-1-5 Kashiwanoha, Kashiwa, Chiba 277-8563 Japan (e-mail: tei.nan@atl.k.u-tokyo.ac.jp).

M. Shino is with the Department of Human and Engineered Environmental Studies, The University of Tokyo, Tokyo, Japan. 5-1-5 Kashiwanoha, Kashiwa, Chiba 277-8563 Japan (e-mail: motoki@sl.k.u-tokyo.ac.jp).

N. Tomokuni is with the Department of Robotics, Kinki University, Takaya Umenobe, Higashi-Hiroshima City, Hiroshima 739-2116, Japan e-mail: tomokuni@hiro.kindai.ac.jp.

G. Murata is with RD Center, JTEKT Corporation, 333 Toichi-cho, Kashihara City, Nara 634-8555, Japan (e-mail: genki_murata@jtekt.co.jp).

II. Related Works

Several EPWs with the ability to climb stairs are developed which use a caterpillar track or wheeled links. Topchair [4] and Scewo[5] are successful examples for EPWs using a caterpillar track. Their compact size allow them to be used both indoors and outdoors. However, because of the combination of wheels for flatland and caterpillars for stairs, they are bulkier and heavier than standard wheelchairs. Another drawback is that it cannot be used on round-edge stairs as well as stairs with high inclination angle. In addition, maintenance is need due to the abrasion of caterpillars and stairs. A wheeled link consists of a rotary link and at least two wheels conbined with the link and researchers generally use two or four wheeled links. Wheelchair.q [6] developed by Politecnico di Torino used two wheeled links in front and another two in the rear. Because of the fixed distance between front links and rear links, stair-climbing is limited for some stair size, and it may not pass the ISO standards [7] for EPWs. By using only two wheeled links, iBot [8] was compact and commercially available at a time. However, when climbing stairs, the user must hold a handrail to keep balance because of its unstable, so that elderly people and those who have an upper limb disability have to recieve help from a caregiver.

III. Previous Studies

A. Design of Mechanism

In previous researches, the authors developed a wheeled inverted pendulum type robotic wheelchair for stair-climbing[9]. As shown in Fig. 1, a rotary link with two wheels at both sides enables the robot to step on the stairs, and a seat slider which can move back and forth enables it to maintain balance. While stepping on the stairs, the position of the center of gravity can be always maintained above the wheel in contact with the ground by using the slider. It is different from the iBot that the adjustment of balance is done autonomous.

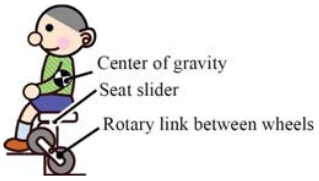

Fig. 1 Inverted pendulum type robotic wheelchair [9]

To climb up and down the stairs, the proposed wheelchair has two control stages: the gravity-center control stage and the wheel-linkage control (inverted pendulum control) stage. The stair-climbing procedure is shown in Fig. 2.

(a)The wheelchair approaches the stairs in wheel-linkage control stage. Next, rotary links are rotated forward until the upper wheels are placed on the step. The seat slider is pulled backward simultaneously to maintain the center of gravity just above the lower wheels.

(b)When the upper wheels contact the step, the wheel-linkage control is turned off and the gravity-center control is turned on. The seat slide is advanced to move the center of gravity from the lower wheels to the upper ones preparing for the next control stage.

(c)The wheel-linkage control is restarted.

(d)The rotary links are rotated until vertical so that the positions of the upper wheels and lower wheels are changed. The seat slider is still moved in this period to maintain balance.

(e)The wheelchair climbs one step. Stair-climbing can be realized by repeating (a) to (e).

At the wheel-linkage control stage, the system is considered as an inverted pendulum. In order to deal with the restriction conditions on the stairs, the seat slider instead of the wheels is used to maintain balance while the wheels are desirable not to move. As shown in Fig. 3, two-degree-of-freedom control is adopted, which consists of a feedforward control to follow the target trajectory and a feedback control to compensate for disturbance.

In the feedback control, the deviation of the state quantity between the measured value and the target value is fed back. The feedback gain K is determined by using the gain schedule value based on linear-quadratic regulator(LQR) theory. In the feedforward control, the target trajectory of state quantities are determined based on the staircase dimensions. It is confirmed that when the time for ascending or descending one step T is longer than 3 seconds, the acceleration of the rider is less than 0.315 m/s^2 so that the rider do not feel uncomfortable [10]. Therefore, the period was set to be 3 seconds in the previous research.

IV. Problems of Previous Researches

In the previous research, the authors have vertified the effectiveness of the mechanical structure and the control strategy for stair-climbing by running a simulation, which uses Open Dynamics Engine(ODE) as the physical calculating engine. Therefore, a prototype wheelchair has been developed. As shown in Fig. 4, the prototype wheelchair has a slider actuator under the seat and rotary links and wheels drive motors. In addition, there is a sensor for each actuator, and an inertial measurement unit (IMU) to measure the pitch angle. Although the showed that the wheelchair successfully overcomes stairs with the proposed control strategy, the prototype wheelchair fell down. The reason is thought to be the lack of considerations of differences between the simulation environment and the real environment.

A. The Differences between Simulation and Real Environment

Generally, modeling errors, sensor noises, actuator errors and gear backlash, etc are considered to be the main differences between simulation and real environment.

1) Modeling Errors: In this research, the authors simplified the real wheelchair model for easy control and no external force is considered. The dimensions, mass, center of gravity and moment of inertia of each joint of the prototype wheelchair may not match the design value. These can be decreased by parameter identification to some extent.

2) Sensor Noises and Actuator Errors: According to M.Shino's experiments [9], the autuators have sufficient frequency response up to 30 Hz, which enables good controllability. The resolution of sensors also satisfies the requirements for control. Therefore, sensor noise and actuator error are ignored in this paper.

3) Gear Backlash: When inverted pendulum control is performed on a staircase, it is necessary to strictly control the wheel position. However, since the reduction drive contains spur gears, there is a wheel positioning error corresponding to the gear backlash between the wheels and the actuator. Even though scissors gears were used in order to reduce the backlash, there is still 0.198°backlash. Backlash also leads to the measurement error of wheel rotation angle and angular velocity. To reduce the measurement error, it is desirable to measure the rotation of the wheel directly. However, it is difficult because of the rotation of rotary links. Therefore, the authors measure the rotation of the motor shaft and convert the wheel rotation angle and angular velocity from the motor angle, which has a measurement error corresponding to the gear backlash and makes the system to be a dead time system. As a result of compensating for this measurement error, it becomes a divergent system. Thus, the wheel position can not be fed back, and the feedback gain of the wheel speed has to be reduced.

B. Avoidance of Falling Down

Due to the modeling error, the slider may not just in the right position to maintain balance and the wheels tend to move insteadly. In case of a small wheel speed feedback gain, wheel movement occurs back and forth. As a result, the wheels slide down the stairs or the wheels collide with the side of the stairs, and finally leads to fall down.

In order to avoid falling down, one method is reducing the back and forth movement of the wheels. Another method is developing a control system which can maintain the balance of the wheelchair when the wheels collide with the stairs. In this research, the authors adopt the method of reducing the back and forth movement of the wheels.

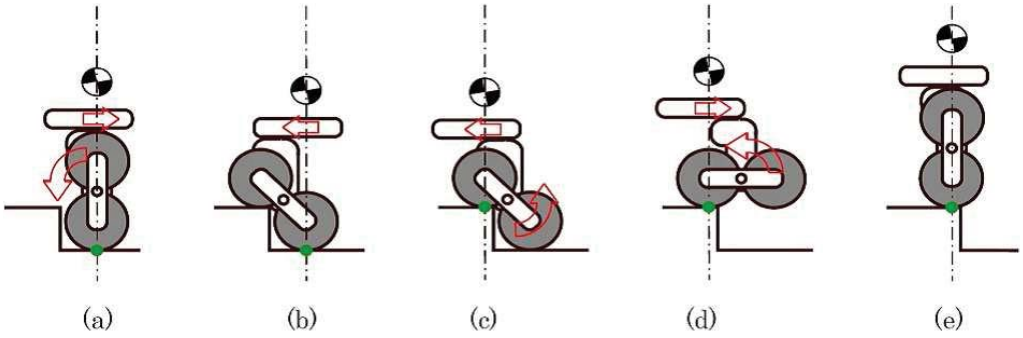

Fig. 2 Sequence to climb stairs [9]

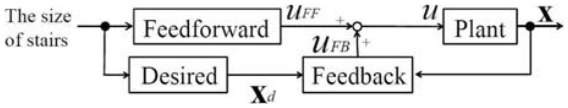

Fig. 3 Control block of developed system [9]

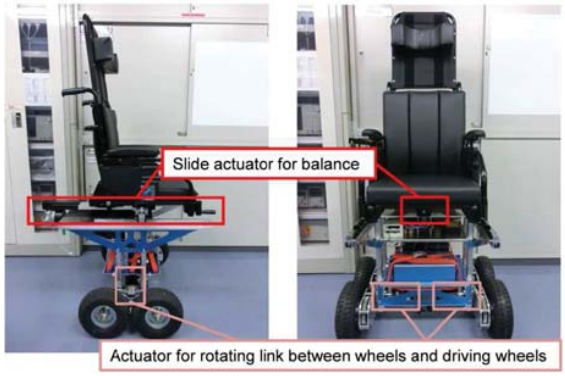

Fig. 4 Appearance of the robotic wheelchair equipped with stair climbing mechanism [9]

Although it is theoretically better to increase the feedback gain of the wheel control, the wheel vibration will diverge and the wheelchair will become unstable due to the gear backlash. Therefore, a control algorithm that can reduce the wheel movement in a low feedback gain condition is necessary.

In this research, the authors proposed a fall avoidance control that reduces the wheel movement by focusing on the wheel speed control under the constraint condition where the wheel position control cannot be performed. The movement of the wheels occurs due to the slider force and the rotational inertia of the rotary links. Therefore, in order to reduce the wheel movement, when the wheel speed feedback gain can not be set high, a method of reducing the deviation of the slider and the rotary links from the target trajectory can be effective.

V. Control Strategy

A. System Modeling

The proposed system is modeled as a three dimension rigid body link model. As shown in Fig. 5, six degrees of freedom are given: the rotation angle of reft wheel θ_{lw}, right wheel θ_{rw}, reft rotary link θ_{ll} and right rotary link θ_{rl}, the position of the seat slider x_s and the pitch angle θ_{bp}. The five inputs are the control torque of the left wheel actuator τ_{lw}, right wheel actuator τ_{rw}, left rotary link actuator τ_{ll}, right rotary link actuator τ_{rl} and the slider actuator F_s.

B. Kinematics Equations

Kinematics equations for control are derivated using the Lagrange's equation. Equation (1)-(5) show Lagrange's equations of wheels, links and the slider.

$$\text{Right Wheel Torque} \quad \tau_{rw} = \frac{d}{dt}\left(\frac{\partial L}{\partial \dot{\theta}_{rw}}\right) - \frac{\partial L}{\partial \theta_{rw}} \tag{1}$$

$$\text{Left Wheel Torque} \quad \tau_{lw} = \frac{d}{dt}\left(\frac{\partial L}{\partial \dot{\theta}_{lw}}\right) - \frac{\partial L}{\partial \theta_{lw}} \tag{2}$$

$$\text{Right Link Torque} \quad \tau_{rl} = \frac{d}{dt}\left(\frac{\partial L}{\partial \dot{\theta}_{rl}}\right) - \frac{\partial L}{\partial \theta_{rl}} \tag{3}$$

$$\text{Left Link Torque} \quad \tau_{ll} = \frac{d}{dt}\left(\frac{\partial L}{\partial \dot{\theta}_{ll}}\right) - \frac{\partial L}{\partial \theta_{ll}} \tag{4}$$

$$\text{Slider Force} \quad F_s = \frac{d}{dt}\left(\frac{\partial L}{\partial \dot{x_s}}\right) - \frac{\partial L}{\partial x_s} \tag{5}$$

Since there is no input on the pitch angle, the equation is represented as (6).

$$0 = \frac{d}{dt}\left(\frac{\partial L}{\partial \dot{\theta_{bp}}}\right) - \frac{\partial L}{\partial \theta_{bp}} \tag{6}$$

C. Control Strategy of Slider

The pitch angle of the wheelchair should be zero, which means that the target trajectory of the seat slider can be obtained by equilibrium of moments, as shown in (7) and (8). The total weight of the wheelchair $(4m_w + 2m_l + m_b + m_s)$ is written as M.

$$x_{sref} = -\frac{1}{2}\frac{Ml}{m_s}\left(\cos(\theta_{rl}) + \cos(\theta_{ll})\right) \tag{7}$$

$$\dot{x}_{sref} = \frac{1}{2}\frac{Ml}{m_s}\left(\dot{\theta}_{rl}\sin(\theta_{rl}) + \dot{\theta}_{ll}\sin(\theta_{ll})\right) \tag{8}$$

However, the slider does not follow the target trajectory well and starts to vibrate, because of the modeling errors and

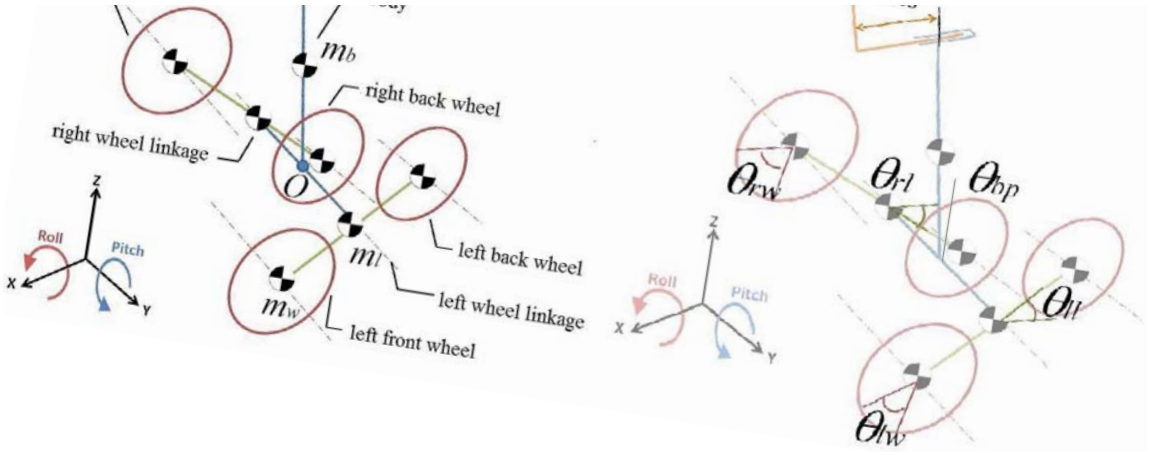

Fig. 5 Mass model

backlash. A control strategy to absorb the vibration of the slider is considered so that the slider force will not transmit to the wheel. The authors proposed a skyhook model as shown in Fig. 6 to add a virtual damper element to the slider. According to the skyhook theory, the actuator force to be generated should be proportional to the deviation of the slider speed as shown in (9).

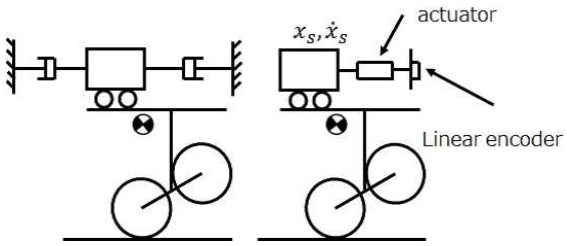

Fig. 6 Skyhook model

$$u_{sky} = k_v \left(\dot{x}_{sref} - \dot{x}_s \right) \tag{9}$$

Considering the extensibility of the control system construction, the target trajectory of the slider speed was newly designed as (10), in order to integrate the feedback input and the skyhook input into the LQR system. K is the damper coefficient, which can be changed arbitrarily.

$$\hat{\dot{x}}_{sref} = \dot{x}_{sref} + K \left(\dot{x}_{sref} - \dot{x}_s \right) \tag{10}$$

In order to grasp the characteristics of K, the amount of wheel movement when giving different skyhook gains was graphed using the ODE simulation. As same as the prototype wheelchair, the simulation was carried out in the conditions without the feedback control of the wheel positions. As shown in Fig. 7, when the control stage switches from the gravity-center control stage to the wheel-linkage control stage, the wheels start to move due to errors of state quantities such as the pitch angle. In the case where only the wheel speed is feedback controlled, that is, when the skyhook gain is zero, the vibration of the wheels starts and diverges in the wheel-linkage control stage. This is considered to be the cause of the falling down of the prototype. When an appropriate skyhook gain is given, the vibration of the wheels disappears and the amount of wheel movement decreases. However, if the gain is too high, it can be seen that the wheels tend to vibrate in the reverse direction. Therefore, the authors selected a gain $K = 1$ that stabilizes the wheel position.

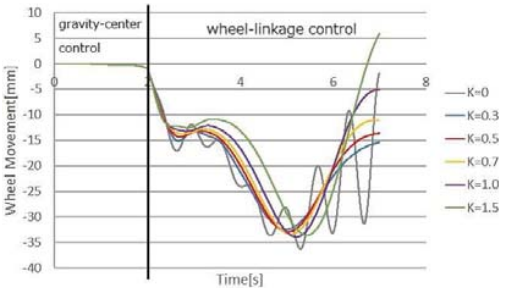

Fig. 7 Relationship between wheel movement and skyhook gain

Although the skyhook control of the slider can be used to absorb the vibration of the wheels, it is not possible to completely eliminate the wheel position deviation.

D. Control Strategy of Wheel Linkage and Wheel

Considering the smoothness of motion, the target trajectory of rotary links is designed using a quintic polynomial interpolation function, as shown in (11) and (12).

$$\theta_{lref} = \frac{10t^3T^2 - 15t^4T + 6t^5}{T^5}\Delta\theta + \theta_0 \tag{11}$$

$$\dot{\theta}_{lref} = \frac{30t^2T^2 - 60t^3T + 30t^4}{T^5}\Delta\theta \tag{12}$$

As shown in (13) and (14), the target trajectory of the wheels must be the reverse of the target trajectory of the rotary links, according to constraint conditions for wheels not to move.

$$\theta_{wref} = -\theta_{lref} \tag{13}$$

$$\dot{\theta}_{wref} = -\dot{\theta}_{lref} \tag{14}$$

When ascending and descending the stairs, the target trajectory of the rotary links and wheels is determined based on the staircase dimensions. Since the wheel radius and the length of the rotary link are constant, the range in which the wheel can move is smaller as the step is higher. Therefore, when ascending or descending stairs with a high step height, the period T should be set long enough to avoid collision or sliding down of the stairs.

When the wheels are in the state shown in Fig. 8, the allowable deviation of wheels can be obtained as (15). In order to ascend or descend the stairs as fast as possible and to secure the movement range in both forward and backward directions at the same time, the initial wheel postion is set to be in the middle of the range when wheel-linkage control stage is started. Thus, the maximun value of the wheel movement is set as (16).

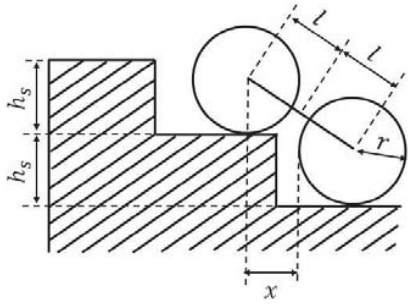

Fig. 8 Wheels and stairs

$$x \leq \sqrt{4l^2 - {h_s}^2} - r \tag{15}$$

$$x_{err} = \frac{\sqrt{4l^2 - {h_s}^2} - r}{2} \tag{16}$$

As shown in Fig. 9, due to the rotational inertia of the rotary links, the wheel position deviation becomes larger as the period of ascending or descending per step is shorter. Therefore, control strategy in the previous research that the period $T = 3$ sec cannot be used.

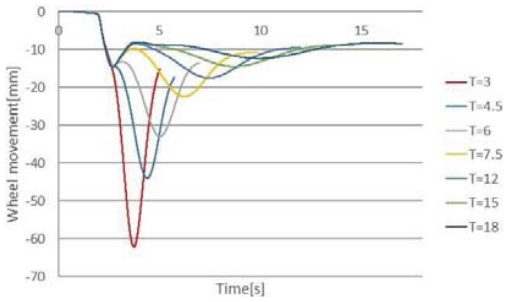

Fig. 9 Relationship between wheel movement and the period for per step

As shown in Fig. 10, in order to obtain the shortest period T within a range that the wheels do not slide down the stairs and do not collide with the side of the stairs, the authors plotted the sets of period and maximum value of wheel movement corresponding to the period in Fig. 9. The shortest period is given as a function of the maximum value of wheel movement (17), by using a polynomial approximation.

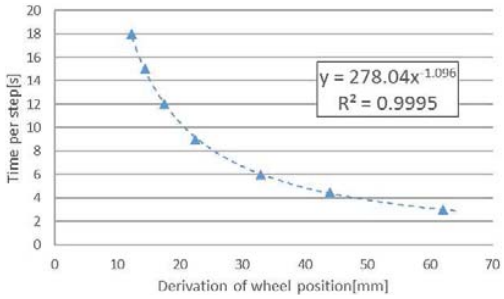

Fig. 10 Relationship between wheel movement and the period for per step

$$T = 278.04\ {x_{err}}^{-1.096} \tag{17}$$

Period T obtained by (17) is used in (11) and (12) to calculate the target trajectory of the rotary link.

E. Feedback Control

A two-degree-of-freedom control is adopted as it was done in previous researches. Design of the target trajectory was described in the preceding section. In this section, the authors will explain how to obtain a feedback control input for compensating for the deviation of the state quantity between the measured value and the target value.

By linearizing the derived kinematics (1)-(6), the state equation is obtained as (18). For linearization, only the first order terms are considered.

$$\frac{d}{dt}\boldsymbol{x}_k = \boldsymbol{A}_{10\times10}\left(\theta_{rl}, \theta_{ll}\right)\boldsymbol{x}_k + \boldsymbol{B}_{10\times5}\left(\theta_{rl}, \theta_{ll}\right)\boldsymbol{u} \tag{18}$$

State quantities $\boldsymbol{x}_k$ and inputs $\boldsymbol{u}_k$ are shown as (19) and (20).

$$\boldsymbol{x}_k = [\theta_{rl}\ \theta_{ll}\ x_s\ \theta_{bp}\ \dot{\theta}_{rl}\ \dot{\theta}_{ll}\ \dot{\theta}_{rw}\ \dot{\theta}_{lw}\ \dot{x}_s\ \dot{\theta}_{bp}]^T \tag{19}$$

$$\boldsymbol{u}_k = [\tau_{rw}\ \tau_{lw}\ \tau_{rl}\ \tau_{ll}\ F_s]^T \tag{20}$$

Based on the LQR theory, a feedback gain $\boldsymbol{K}_x$ which minimizes the evaluation function (21) is derived.

$$J(t) = \int_0^\infty [\boldsymbol{x}^T(t)\boldsymbol{Q}\boldsymbol{x}(t) + \boldsymbol{u}^T(t)\boldsymbol{R}\boldsymbol{u}(t)]dt \tag{21}$$

Q is the weighing matrix of the control state quantity and R is the weighing matrix of the control input. Diagonal matrices are shown as (22) and (23).

$$\boldsymbol{Q} = diag[20000, 20000, 10000, 250000, 50, 50, 5000, 5000, 50, 50] \tag{22}$$

$$\boldsymbol{R} = diag[2, 2, 1, 2, 2] \tag{23}$$

The feedback control input is calculated by the control law based on the derived feedback gain, as shown in (24). $\boldsymbol{u}_k$ is the sum of the LQR input in previous researches and the proposed skyhook input in this paper.

$$\boldsymbol{u}_k = \boldsymbol{K}_x\left(\boldsymbol{x}_{kref} - \boldsymbol{x}_k\right) \tag{24}$$

F. Control Block Diagram

The control block diagram of the proposed control strategy is shown in Fig. 11. The control stategy of the previous research is surrounded by a red line. In this research, the authors determined the target trajectory of state quantities not only based on the staircase dimensions, but also based on the measured value of them. $G1$ is the expression for (11)-(14), which determines the target trajectory of the rotary links, $G2$ is the expression for (10), which determines the target trajectory of the slider. K is the feedback gain of the skyhook control.

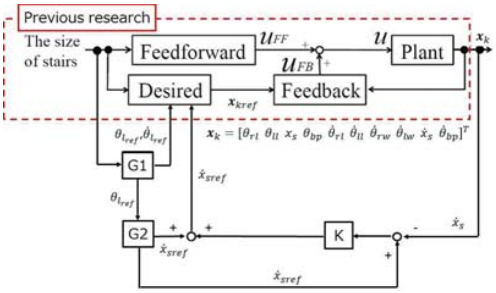

Fig. 11 Control Block Diagram

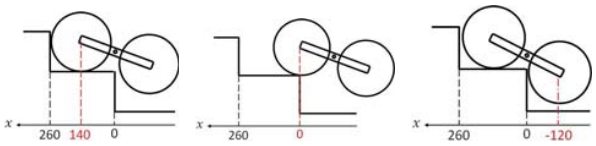

(a) boundary conditon 1 (b) boundary condition 2 (c) boundary condition 3

Fig. 12 Fall down boundary conditions

VI. Validation of Control Strategy

In order to evaluate the effectiveness of the proposed fall avoidance control strategy, ODE simulations and experiments were conducted.

A. Simulation Conditions

Since this wheelchair was designed to correspond to the staircase dimensions that satisfy the Building Standards Law [11], the simulation was carried out under the conditions of the step length of 260 mm and the step height of 120 mm, 150 mm, and 180 mm, respectively. The period of ascending per step was calculated using (17) and summarized in TABLE I. For the purpose of comparison, a simulation was carried out with control strategy of the previous researches. In this case the step height was set to 180 mm.

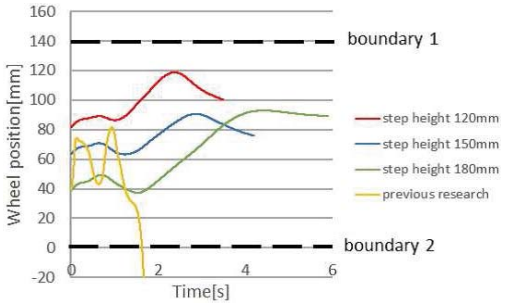

Fig. 13 Time history of the upper wheels position during the wheel-linkage control stage

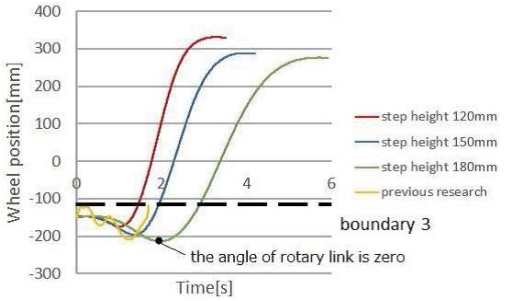

Fig. 14 Time history of the lower wheels position during the wheel-linkage control stage

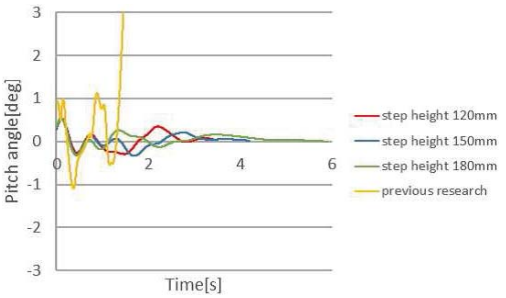

Fig. 15 Time history of the pitch angle during the wheel-linkage control stage

TABLE I
Stair Step Height and Period per Step

Stair step height h_s	Period of per step T
120 mm	3.5 sec
150 mm	4.2 sec
180 mm	5.9 sec

B. Simulation Results

In order to validate the effectiveness of the fall avoidance control, if any collision or slide down occurs or not was evaluated from the amount of the wheel movement, and the stability was evaluated from the pitch angle. As shown in Fig. 12, there is a boundary condition 1 where the upper wheels (wheels in contact with the ground) collide with the side of the stairs, a boundary condition 2 where the upper wheels slide down the stairs and a boundary condition 3 where the lower wheels(wheels free from the ground) collide with the side of the stairs. In order to avoid collision or slide down, the position of the upper wheels must be between the boundary condition 1 and 2, and the lower wheels must do not reach the boundary condition 3 until the rotary links rotate to the horizontal angle.

Figs. 13-15 show the time history of the upper wheels position, the lower wheels position and the pitch angle during

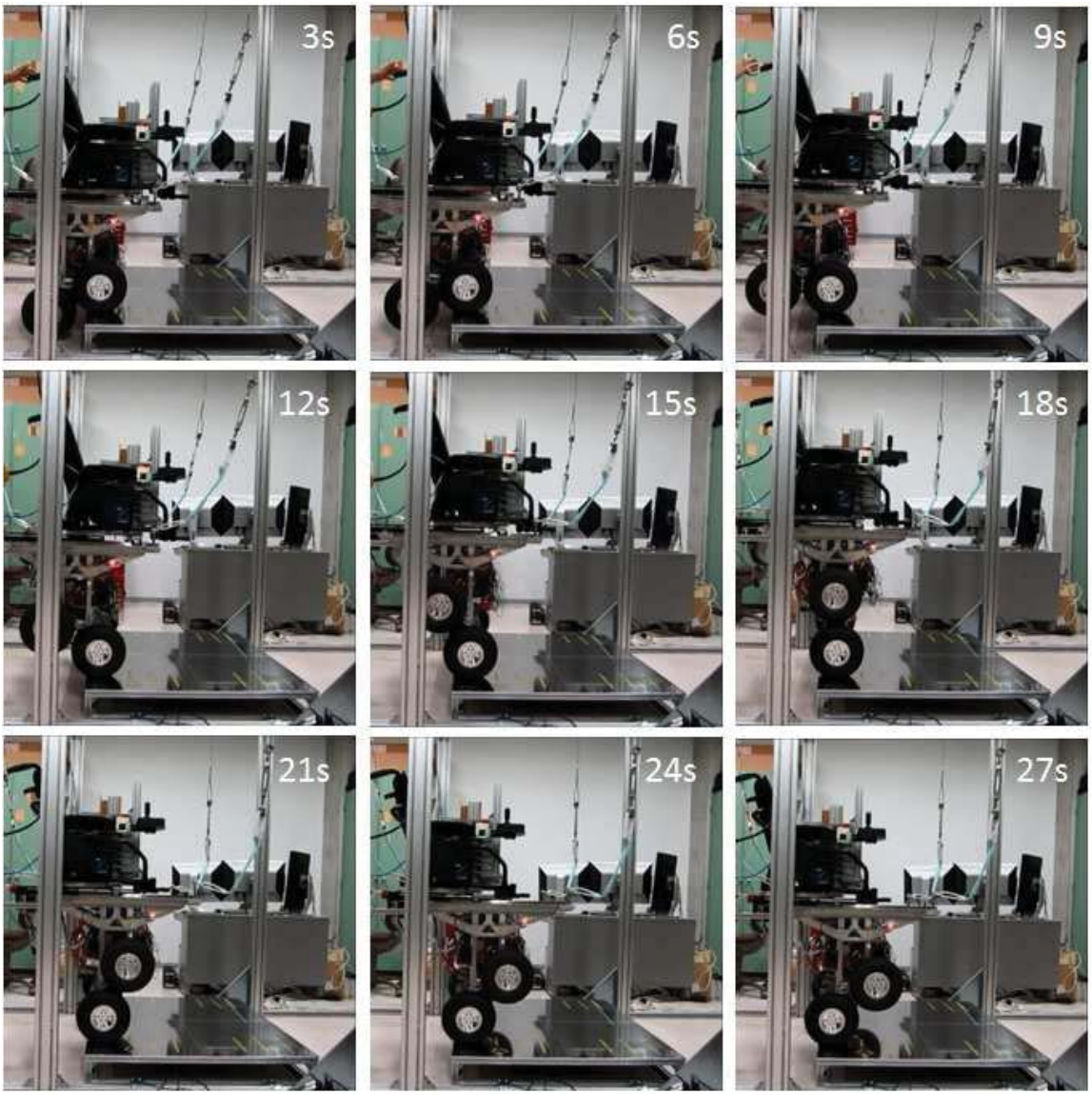

Fig. 16 Time History Images with Proposed Control Strategy during Stair Climbing

the wheel-linkage control stage. As shown in Fig. 13, the upper wheels slide down the stairs in previous control conditions. However, they lie within the boundary in the proposed control conditions. According to the geometric relationship of the wheelchair, when the rotary links reach the horizontal angle, the position of lower wheels shows the minimum value. As shown in Fig. 14, in previous control conditions, the wheels collide with the side of the stairs. In the proposed control conditions, collision does not occur. As shown in Fig. 15, by using the control strategy proposed in this paper, the pitch angle of the wheelchair is within 0.5 degree, which shows that the wheelchair does not fall down and has a good stablity.

Based on the results shown in Figs. 13-15, it was confirmed in the ODE simulation environment that using the controller proposed in the this research, the wheelchair is possible to rise the stairs without colliding with the side of the stairs, or sliding down the stairs, and in a stable posture.

C. Experiment Conditions

In order to confirm the fall avoidance effect of the proposed control in the real environment, experiments were conducted to raise a 14 cm high step using the prototype wheelchiar. The period T was set to be 30 sec.

D. Experiment Results

It was confirmed that the prototype wheelchair rises one step with the probability of 80%. The state at that time is shown in Fig. 16. It means that the control stategy of the stair climbing wheelchair proposed in this research is effective to reduce the movement of wheels and reduce the probability of falling. However, the rest 20% collided with the side of

the stairs or slided down the stairs, and the wheelchair falled down. It is conceivable that the reason of falling down is that the influence of modeling error and backlash is much larger than expected.

VII. Conclusion

It became clear that the lack of wheel position feedback control due to the gear backlash as well as modeling errors causes the wheel movement, and finally causes the falling down of the prototype wheelchair. In order to avoid falling down, the authors focused on wheel speed control and proposed a control strategy to reduce the amount of wheel movement. Four major conclusions were obtained.

- A new target trajectory of the seat slider was considered based on the skyhook theory, in order to reduce the vibration of wheels by reduce the slider force.
- In order to limit the amount of wheel movement within the range that the wheelchair does not fall down, the shortest period of ascending or descending per step was set corresponding to the staircase dimensions.
- It is verified in the ODE simulation condition that the proposed control strategy is applied to the staircase dimensions that satisfies the Building Standards Law.
- The prototype wheelchair can rise one step with the probability of 80%. However, since the modeling errors and backlash are much larger than expected, the wheelchair could only rise the step with a low speed, instead of the shortest period of per step.

Acknowledgment

This research is supported by JTEKT Co.Ltd.

References

[1] Cabinet Office, Government of Japan, the handicapped white paper, 2015.
[2] U.S. Access Board Washington, DC, Demographics of Wheeled Mobility Device Users. In Conference on Space Requirements for Wheeled Mobility, 2003.
[3] Americans with Disabilities Act Accessibility Guidelines (ADAAG), https://www.access-board.gov/guidelines-and-standards/buildings-and-sites/about-the-ada-standards/guide-to-the-ada-standards (12/7/2016 accessed).
[4] Laffont I, Guillon B, Fermanian C, Pouillot S, Boyer F, et al. *"Evaluation of a stair-climbing power wheelchair in 25 people with tetraplegia"*, Arch Phys Med Rehabil 2008; 89(10): 1958-64.
[5] ETH Zurich, The Stairclimbing Wheelchair Scewo, http://scalevo.ch/ (12/7/2016 accessed).
[6] Quaglia G, Franco W, Oderio R, "Wheelchair.1, a mechanical concept for a stair climbing wheelchair", Robotics and Biomimetics (ROBIO) IEEE International Conference, pp.800-805.
[7] ISO standard: Wheelchair - Section 5: Determination of dimensions, mass and maneuvering space ISO 7176-5.
[8] Unstal H, Minkel JL, *"Study of the Independence IBOT 3000 Mobility System: An Innovative Power Mobility Device, During Use in Community Enveronments"*, Arch Phys Med Rehabil 2004; 85(12): 2002-10.
[9] M. Shino, N. Tomokuni, G. Murata and M. Segawa, *"Wheeled Inverted Pendulum Type Robotic Wheelchair with Integrated Control of Seat Slider and Rotary Link between Wheels for Climbing Stair"*, 2014 IEEE Workshop on Advanced Robotic and its Social Impacts (ARSO), 2014, pp121-126.
[10] JIS B 7760-2:2004 (ISO 2631-1:1997) whole-body vibration Part 2: General requirements for measurement for measurement and evaluation method.
[11] Enforcement Ordinance of Construction Standard Law, Articles 23-27.